Vol. 38 No. 3 Journal of the Communications Research Laboratory November 1991
Printed in Tokyo, Japan pp. 435 – 457

III. VLBI SYSTEM

III.2 K-3 AND K-4 VLBI DATA ACQUISITION TERMINALS

By
Hitoshi KIUCHI, Shin'ichi HAMA, Jun AMAGAI, Yuko ABE, Yuji SUGIMOTO, and Noriyuki KAWAGUCHI

(Received on March 18, 1991)

ABSTRACT

A new data acquisition system, K-4, is developed by the Communications Research Laboratory (CRL), Japan as the next generation VLBI system. We have previously developed K-1, K-2, K-3 VLBI systems and the K-3 system succeeded in measuring plate motion. The K-4 system uses a rotary-head cassette recorder that makes the system smaller and easier to operate. The K-4 system is a compact VLBI terminal, one forth the weight and one fifth the size of the Mark-III and K-3 systems. The K-4 system can be made fully compatible for output data from the Mark-III and the K-3 VLBI systems by using Input and Output Interface Units. The measured coherence loss of both the K-4 and the K-3 system is less than 5%. This shows that both systems perform well enough for VLBI experiments. It is found that the geodetic results for the 55 km baseline (Kashima-Tsukuba) of the K-4 system agree with those of the K-3 system, with a vector discrepancy of only a few millimeters. In 1990 this system obtained good geodetic results in Antarctica.

1. Introduction

In the Very Long Baseline Interferometer (VLBI)[(1)-(4)], the radio emission from a radio source several billion light years away is received by two stations and the distance between the two stations can be determined with an accuracy of 1–3 cm by measuring the slight difference in arrival times of the signals at the two stations. As the received radio wave is very weak, it is necessary to integrate a very large amount of data. Hence, it is necessary to record a large amount of observational data. A high-recording density high-speed large-capacity data recorder is therefore one of the most important parts of the VLBI system. The K-3 system used a fixed-head digital video recorder with open real tape. The K-3 system was designed for general purpose VLBI, geodesy, astronomy etc. It is usually operated as a fixed station. Due to the development of technology, VLBI is now used for more varied purposes and its observing stations are not only fixed ones but mobile ones used in remote islands and in Antarctica. As Japan excels in the technology of the rotary-head type recorder, in K-4 system uses a rotary-head digital-data cassette recorder. This satisfies the demand for a mobile observation system which is easy to transport, set-up, and operate.

2. The K-3 System

CRL developed the K-3 VLBI system at Kashima in accordance with the five-year plan (1979–1983)

and completed it in October 1983. On November 5, 1983 the first transpacific VLBI experiment conducted between Japan and the United States of America (Mojave and Owens Valley) resulted in a precision of 0.1 nsec in determining the delay time as had been expected. On January 23 and February 25, 1984 system level experiments were completed in cooperation with Mojave and Hat Creek. The data processing and analyses made at CRL and at NASA showed that the K-3 system achieved a precision of better than 3 cm for the baseline length. This matched the fundamental goal of system performance. The K-3 system will be used for the Japan-U.S. joint experiment starting in July 1984, to measure crustal plate movement with a precision of better than 3 cm. It has also been used for precise time comparison using VLBI[5],[6] between Kashima and Richmond, measurement of the earth rotation, and a domestic VLBI experiment with the Geographical Survey Institute of the Ministry of Construction. K-3 is a precision VLBI system with a variety of applications such as geodesy, astrometry, radio astronomy, etc. It is compatible with the Mark-III VLBI system[7] developed in the U.S.A. Figure 1a shows the K-3 VLBI system front panel. A block diagram of the system is shown in Fig. 1b. The K-3 system is consists of an IF distributor, 14 video converter units, formatter, decoder and recorder. The IF distributor distributes the IF signal to the video converters. The video convertor extracts the desired signal from the IF signal using single side-band frequency conversion. The formatter quantizes (1-bit) the 14-channel video input digital signal with a clock label. The decoder monitors the error rate of the recorded data.

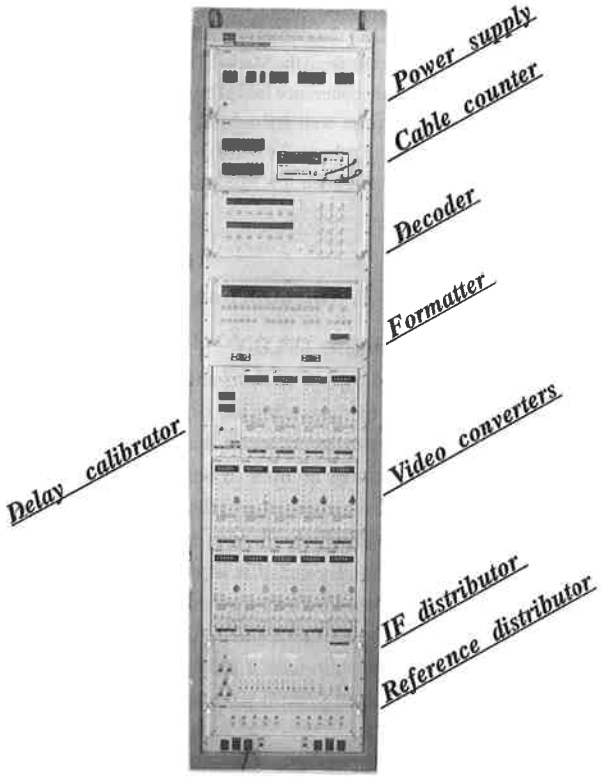

Fig. 1a Front panel of K-3 system.

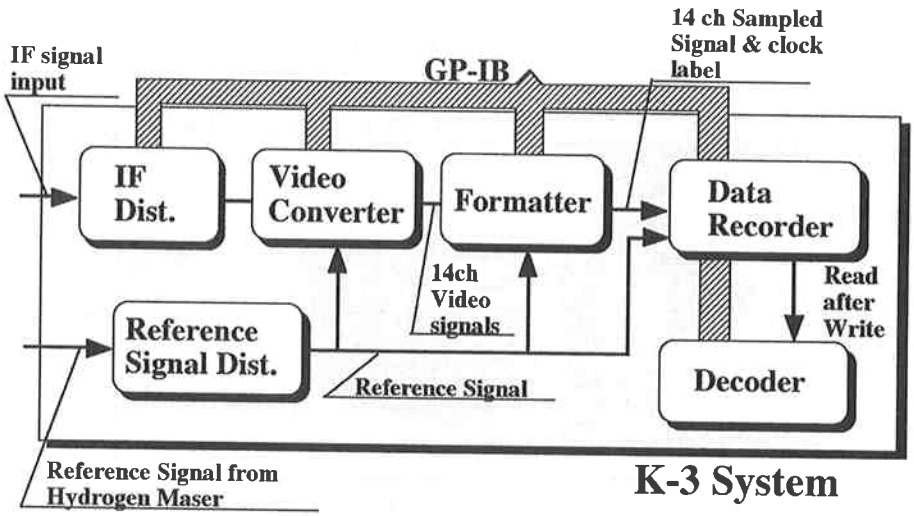

Fig. 1b K-3 system block diagram.

3. The K-4 System

The K-4 VLBI system is being developed at CRL as the next-generation system. In this system a rotary-head cassette recorder (American National Standard 19 mm Type ID-1 Instrumentation Digital Cassette Format) is used to make the system smaller and easier to operate. The interfaces are designed to be compatible with that new recorder. Two interface units are used to obtain compatibility with other VLBI equipment: an input interface unit between the video converter and the recorder and an output interface unit between the recorder and the data processing system. We are making a more compact system with observational functions and data processing functions housed in separate units. The K-4 system consists of the following;

(1) local oscillator
(2) video convertor
(3) input interface unit
(4) output interface unit
(5) data recorder.

Figure 2a shows the K-4 system front panel. The block diagrams are shown in Figs. 2b and 2c.

The local oscillator synthesizes the local frequency signal for the video convertor.

The video convertor converts a window in the IF signal (100–500 MHz) input to a video signal (0–2 MHz). The frequency conversion is achieved by the image rejection mixer using single-sideband conversion. These functions are equivalent to the IF distributor, video convertors (16 ch) and reference distributor of the Mark-III or K-3 VLBI systems.

The input interface unit is used for data acquisition and recording at the VLBI observing station (Fig. 2b). It samples the video signal from the video converter, and sends the digital data to the data recorder together with the time data which is derived from the external time standard signal.

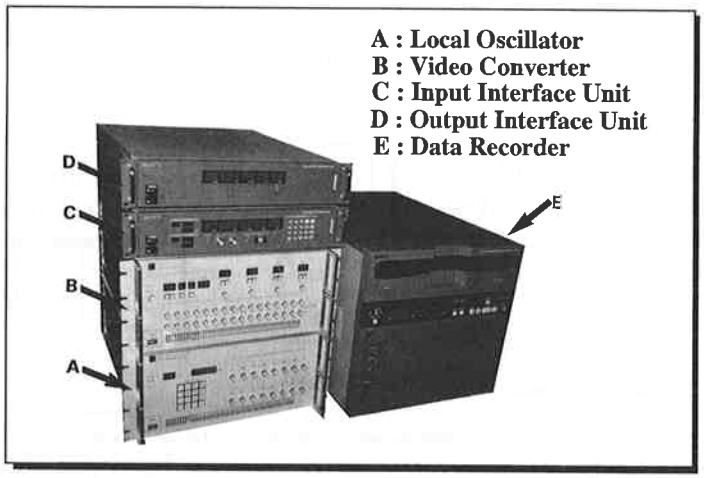

Fig. 2a Front panel of K-4 system.

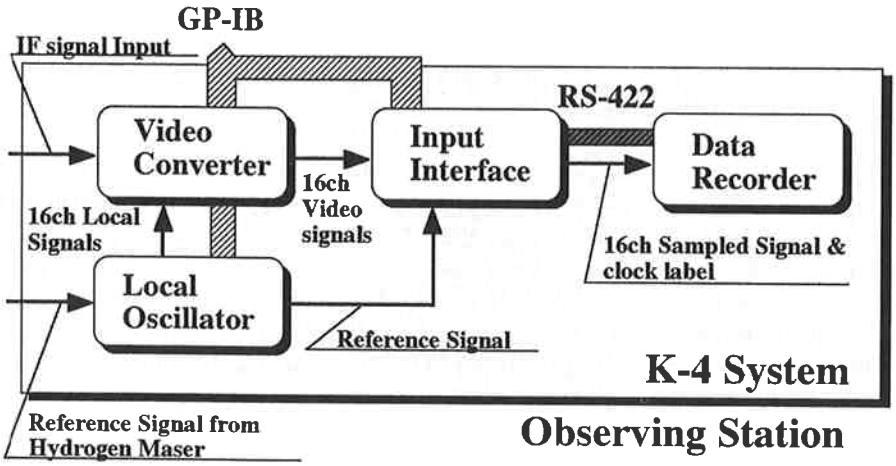

Fig. 2b K-4 system block diagram (observing station).

The output interface unit is used at the correlation station (Fig. 2c). It converts the reproduced data into the appropriate output format, and sends them to the correlator. The format of the output interface unit is compatible with the Mark-III format. Besides this format, another format is also provided for future correlator systems; this provides only digitized raw data signals. When multi-baseline correlation is processed, all the output interface units are daisy-chained through GPIB, so that the tape position data and status data of all the data recorders can be exchanged. The main (reference) output interface supplies the timing clock to sub-output interfaces. The delay bit between the main and sub-output interface units is

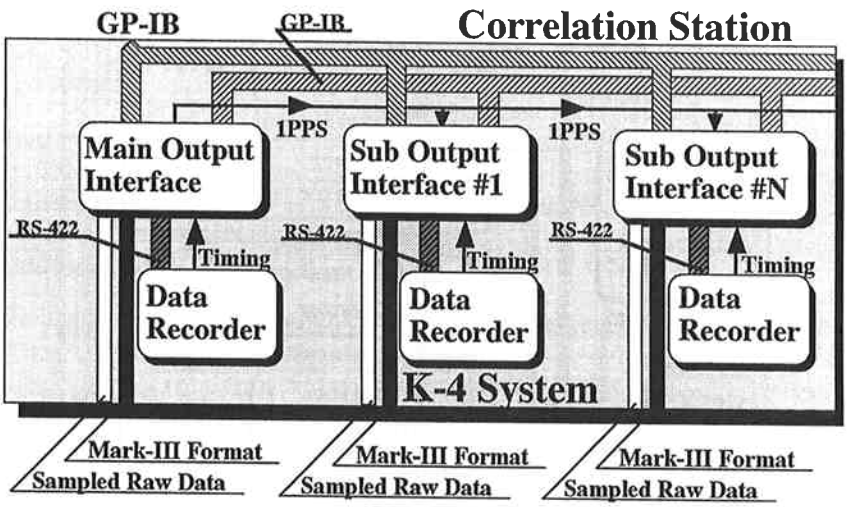

Fig. 2c K-4 system block diagram (correlation station).

Table 1 Size of K-3 and K-4 VLBI data acquisition equipment

K-3 System	size in mm W,H,D		weight in kg
Ref. distributor	426x 95x450		6
IF distributor	426x 199x450		16
Video Converter	85x 262x550	(x14)	119
Formatter	426x 195x450		13
Decoder	426x 195x450		20
Power supply	426x 390x550		37
Data Recorder	560x1650x737		250
Total			461

K-4 System	size in mm W,H,D	weight in kg
Local Oscillator	480x199x590	36
Video Converter	480x199x590	35
Input Interface	424x 88x550	13
Output Interface	424x 88x550	13
Data Recorder	436x432x635	67
Total		164

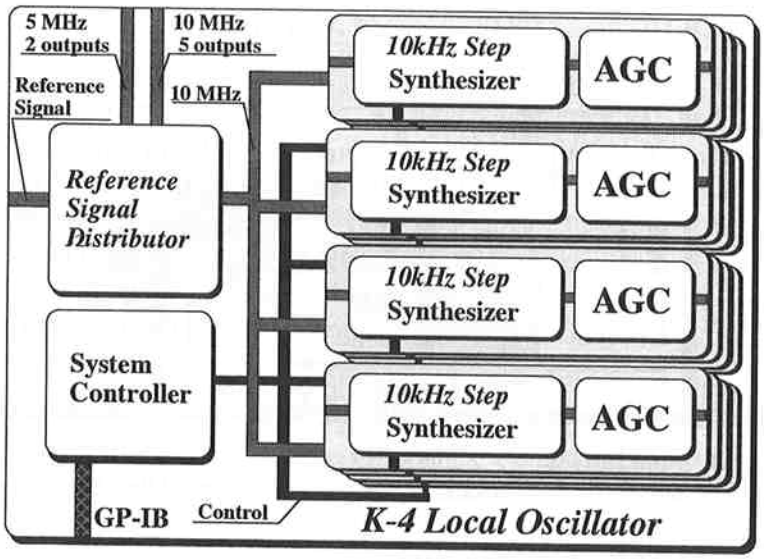

Fig. 3 Local oscillator block diagram.

calculated in each sub-output interface unit, using the time data which is periodically inserted into the recorded data.

It is possible to interface with current VLBI systems through the above-mentioned two interface units. Input and output interface units, when connected together directly, also perform a function equivalent to the formatter of the K-3 VLBI system.

Table. 1 shows the size of the K-4 system compare to the K-3 system. The K-4 is a compact VLBI terminal, one forth the weight and one fifth the size of the Mark-III or K-3 systems.

The next section deals with the data acquisition parts of the K-4 system: local oscillator, video converter, input Interface. III. 3 of this issue deal with the data processing functions for correlation: output interface and data recorder.

3.1 Local Oscillator

This unit is used at the VLBI observing station, and consists of the following sections;

(1) reference signal distribution section
(2) 10 kHz step synthesizer (& auto gain controller) section
(3) system controller.

The block diagram is shown in Fig. 3.

The local oscillator is specially designed for use with the K-4 video converter. It supplies frequency and phase references to the converter which extracts video signals (bandwidth: 2 MHz or 4 MHz) from the IF signal which ranges from 100 MHz to 500 MHz.

The local oscillator outputs sixteen local signals, the frequency of which can be set by local or remote control. The frequency range and the frequency step are fully compatible with conventional VLBI systems such as the Mark-III or the K-3 systems. Communications with a computer for the remote control are made through a standard GP-IB interface. User-friendly message words are used for the communication.

(1) Reference signal distribution section

Geodetic VLBI achieves precise results by using the bandwidth synthesis method[8]. It is necessary to distribute the reference signal (10 MHz) from the hydrogen maser in a way which maintains coherence in each 10 kHz step synthesizer. The coherent 5 MHz signal is made from the 10 MHz reference and is required for the phase calibrator. This section has five 10 MHz outputs and two 5 MHz auxiliary outputs.

(2) 10 kHz step synthesizer section

The 10 MHz reference signal from the reference signal distribution section is divided and its phase is compared with the divided VCO signal, whose frequency is controlled by the CPU in the system controller. The output signal frequency can be selected in 10 kHz steps. This section supplies the local signals which are phase locked to the reference signal and are stable in phase noise. The frequency can be set in the range from 100 MHz to 500 MHz. Usually, this frequency is selected by the experiment organizer, according to the minimum redundancy theory of the bandwidth synthesis. Since the phase calibration signal is constructed every 1 MHz as an IF signal, it must be converted to 10 kHz as a video signal by the synthesized local signal before detection in 10 kHz by the correlation processor. The IF signal range is covered by two VCOs in this synthesizer. The output of the VCO is protected from the influence of the load impedance by an automatic gain controller.

(3) System controller

Execution commands and status data are sent to the host computer through GPIB. The local frequency is set by the computer through GPIB. The device addresses of GPIB are set by the DIP switches.

Table 2 Specifications of local oscillator

SPECIFICATIONS of Local Oscillator	
Output frequency	99.99 to 500.09 MHz in a 10 kHz steps
Output level	+10 dBm
Harmonic ratio	< -30 dB
Spurious ratio	< -40 dB
Phase stability	< 3 deg. with a change of 1 deg. C < 1 deg. with a 1% change of power supply voltage < 3 deg. in Allan variance phase noise at 1sec.
Input reference	10 MHz, +10 dBm
Reference distribution	10 MHz, +10 dBm 5 channels 5 MHz, +10 dBm 5 channels
Remote control	IEEE-488 (GP-IB)
Power supply	100/120/220/240 V AC, 50/60 Hz, 320 VA
Size	480(W)x199(H)x590(D) mm
Weight	36 kg

3.2 Video Convertor

This unit is used at VLBI observing stations, and consists of the following sections;

(1) power detector and attenuator
(2) filter and amplifier
(3) image rejection mixer (IRM) section
(4) system controller.

The block diagram is shown in Fig. 4.

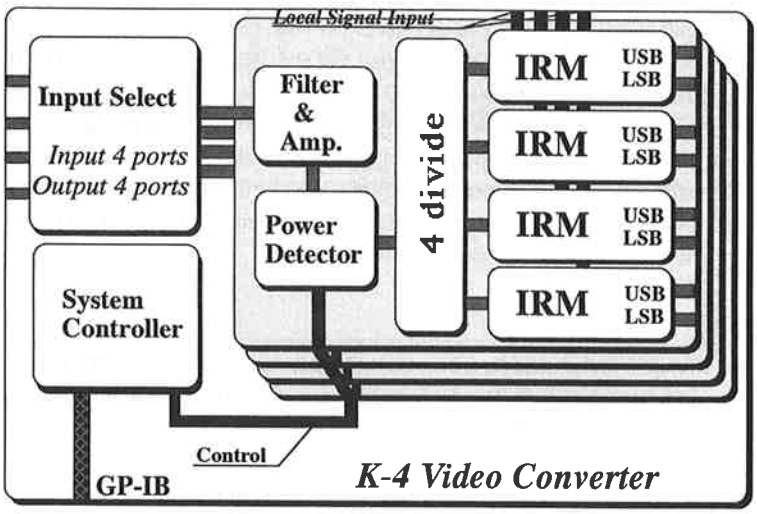

Fig. 4 Video converter block diagram.

The video converter is a compact unit in which an IF distributor and sixteen single side band converters are assembled. All analog devices required in VLBI observations make use of the local oscillator section 3.1. In conventional VLBI systems such as the Mark-III or the K-3, all these units are separated and rack mounted. It is very easy to transport the K-4 unit to a VLBI site and to operate it. Communication with this unit can be made with a computer using user-friendly words through a GP-IB interface.

Two types of operation are supported: one IF input and 16 video outputs; two IF inputs and two groups of outputs. In addition, four IF inputs and four groups of four video outputs are available for dual frequency bands and dual polarization VLBI observations. The video outputs are fully compatible with the Mark-III and the K-3 systems.

(1) Power detector and attenuator

Power detection of the four input IF signals is dealt with in this section. Each IF input signal is divided into four channels. Their powers are detected and sent to the system controller section and displayed on the front panel. The operator sets the attenuators from 0 to 15 dB, in order to keep the detected (displayed)

value between 10 to 90 on the front panel. Linearity is guaranteed within this range.

(2) IF filter and amplifier

Two kinds of band pass filter are included in each channel. One filter has a pass band of 100–230 MHz and the other has 200–520 MHz. The role of these filters is to eliminate 3rd order harmonics from the local oscillator. It is possible to select the Lo-IF or Hi-IF filter from the front panel in local mode or from the host computer in remote mode.

(3) Image rejection mixer (IRM) section

Image rejection mixers are integrated networks composed of an in-phase power divider, two double-balanced mixers and two 90-degree quadrature hybrids (or ±45 degree networks). The primary function of the circuit is to separate the desired signal from its image signal. The image occurs during mixing when both the sum and difference output signals appear in the video band. In the image rejection mixer the image (undesired) signal is separated from the desired signal by vector subtraction. In K-4, this ratio is better than 20 dB.

These low pass filters are located after the IRM section. The filter consists of a 7-pole Butterworth filter circuit, as in the Mark-III and K-3 VLBI systems. The location of the 3 dB point is selected by 91% of the video band maximum frequency. The coherence loss resulting from the imperfect bandpass shape and foldover is about 3% (see Sections 4 and 5).

(4) System controller

Execution commands and status data are sent to the host computer through GPIB. Input attenuator adjustment and IF filter selection are possible remotely from the host computer; the power detected value is sent to the host computer through GPIB. The device addresses of GPIB are set by the DIP switches.

Table 3 Specifications of video converter

SPECIFICATIONS of Video Converter	
IF input	
Number of input IF channels	1/2/4 selectable
Frequency range	100 - 500 MHz
Input level	-45 to -30 dBm/MHz
Input impedance	50 ohm
Video outputs	
Number of video channels	16 (divisible to 4 groups)
Frequency range	0.8kHz - 2 MHz (4MHz option)
Image Rejection Ratio	> 20 dB
Output level	-2.6 dBm/MHz
Local signal leakage	< -50dBm
Output impedance	50 ohm
Remote control	IEEE-488 (GP-IB)
Power supply	100/120/220/240 V, 50/60 Hz, 320 VA
Size	480(W)x199(H)x590(D) mm
Weight	35 kg

3.3 Input Interface Unit

This unit is used at the VLBI observing station. It consists of the following sections;

(1) Sampling section
(2) Time code generator
(3) Phase calibration signal (Pcal) detector
(4) Data recorder interface
(5) Software control section.

The block diagram is shown in Fig. 5.

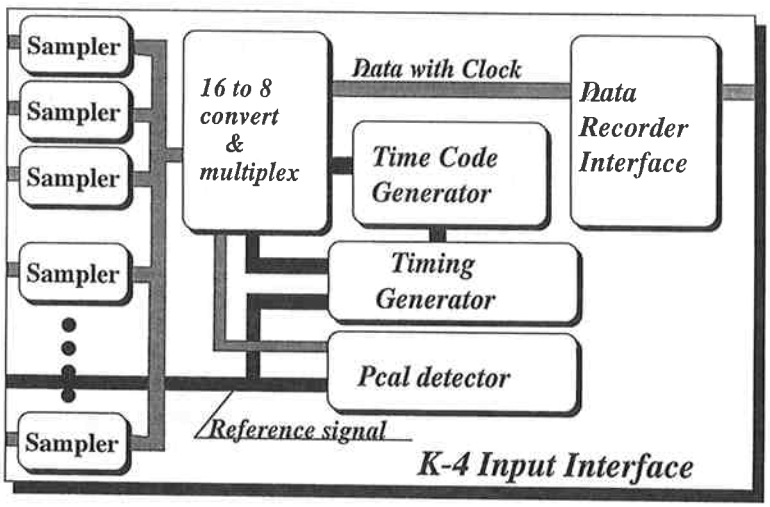

Fig. 5 Input interface block diagram.

(1) Sampling section

This section quantizes (1-bit) the 16-channel 2 MHz (4 MHz) video-bandwidth input signal with a 4 MHz (8 MHz) clock, and produces a 64 Mbps (128 Mbps) data train.

(2) Time code generator

This section produces all the clock signals necessary for the interface and the time data using the 10 MHz standard frequency signal supplied by the hydrogen maser atomic frequency standard and the external 1 PPS signal which is the basis of the UTC time. The time data are backed up by a built-in battery.

The phase of this internal 1 PPS signal is always compared with the leading edge of the external 1 PPS signal, and the error is generally within ±3 clock lengths in terms of the 10 MHz clock. An alarm occurs if the error exceeds that criterion. The status can be sent to the host computer through GPIB.

The time data are generated from the internal 1 PPS signal. They are in the form of YYDDDHHMMSS (BCD), and are overwritten upon the data train every second.

(3) Phase calibration signal (Pcal) detector

This section measures the amplitude and phase of the 10 kHz phase calibration signals, which are included in the video signals, by product-detecting them with a set of phase-quadrature 10 kHz signals which are derived from the external 10 MHz reference signal (Fig. 6). Any 2 channels out of 16 channels are selected for monitoring. They can be selected from the host computer or from the panel. Amplitude is displayed in % and phase is displayed in degrees. The measured data can be sent to the Host Computer through GPIB.

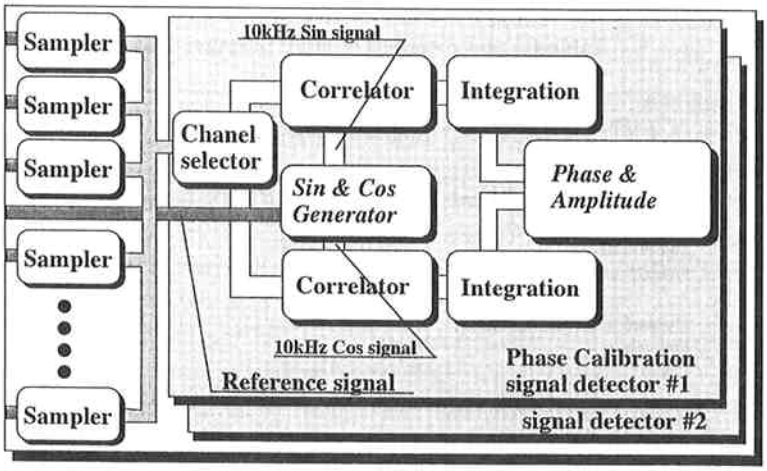

Fig. 6 Pcal detection.

(4) Data recorder interface

The signal data train of the 16 channels sent from the sampling section has a 16-bit format. This data output section translates into an 8-bit format and adds the time data and a (4-byte) sync code. The logic level is converted from TTL to ECL.

(5) Software controlling section

The following controls are performed by the mounted CPU (Z80).

(i) Interface with the host computer

Execution commands and status data are sent to the host computer through GPIB. The device addresses of GPIB are set by the DIP switches in the Input Interface Unit. The functions are;

a) interpret the commands from the host computer
b) control the data recorder accordingly
c) send the status data (time data, phase calibration data)
d) status data of the data recorder back to the host computer.

Also to transfer the protocol errors, device alarm of the data recorder, and status of the data recorder to the host computer through SRQ.

(ii) Interface with the data recorder

The remote control of the data recorder, the status of the operations and error status are exchanged through the RS-422 interface.

It is possible to read the error rates of the data recorder during recording and replaying; and it is possible to send those data to the host computer. The data recorder records a signal which indicates the tape position (23-bit binary data) as well as the sampled data, and the remote control of its set/reset is possible. The recorded position data (ID NUMBER) can be read.

Table 4 Specifications of input interface unit

SPECIFICATIONS of Input Interface Unit	
Input signal	16 channel video signal
Band width of the video signal	2 or 4 MHz, 0 dBm (50 ohm)
Quantization rate	1 bit/sample
Sample rate	4 or 8 MHz/channel
Overall data rate	64 or 128 Mbps
External reference signal	
Frequency	10 MHz
Level	+10 dBm (50 ohm)
External 1 PPS	
Level	TTL compatible (50 ohm)
Build-up time	20 nsec.
Remote control	IEEE-488 (GP-IB)
Power supply	100-120/220 - 240 V, 50/60 Hz, less than 100W
Size	244(W)x 88(H)x550(D) mm
Weight	10 kg

4. Coherence Estimation[9]–[11]

In this section, we discuss the coherence loss of the VLBI system. The fundamental circuit design of K-3 and of K-4 is almost the same. The estimated coherence loss is also about the same for both systems. The cause of the coherence loss is as follows;

1) Reference signal distribution
   i) Phase noise
2) IF signal distribution
   i) Amplifier noise (displayed by noise figure)
3) Video conversion
   i) Image leakage (displayed by image rejection ratio)

ii) Phase noise of local signal
iii) Imperfect band pass
iv) Aliasing noise
4) Sampling
i) Hysteresis and offset.

1) Reference signal distribution

The reference signal supplied from the H-maser must be distributed with coherence maintained to all devices. It is possible to ignore the coherence loss (less than 0.01%) of the reference distribution part from the measurement of phase noise.

2) IF signal distribution

The cause of coherence loss in IF distribution is additional noise from the amplifier. It is possible to measure the performance of the amplifier using the noise figure (NF) and gain given by the NF (Noise Figure) meter. Precision of the NF meter is 0.01 dB for noise figure and gain, and the accuracies are ±0.1 dB for noise and ±0.2 dB for gain. The value obtained is better than 6 dB for noise. This value is –108.5 dBm/MHz in noise power density at the input port of the IF amplifier. The amplified noise power density from the sky is -57 dBm/MHz (typically), so the aggregate of S/N can be ignored (better than 0.01%). Therefore, the coherence loss caused by IF distribution is negligible.

3) Video conversion

i) Image leakage (displayed by image rejection ratio)

The coherence loss of imperfect image rejection is a loss of cross talk from the opposite sideband. If the output signal is U', the upper side band of the input signal in IF is U, the lower side band of the input signal is L, and the coupling coefficients are k and x; then U' is given by the followings:

$$U' = kU + xL.$$

The signal power is given by:

$$\langle U'^2 \rangle = k^2 \langle U^2 \rangle + x^2 \langle L^2 \rangle + 2kx\langle UL \rangle$$

where < > denotes time average.

Assuming that U and L are independent of each other, and that they are random noise, then <UL> is zero. If the restrictions in power are uniform for U, L, U' and L', then x is described by $\sqrt{1-k^2}$. Hence

$$U' = kU + \sqrt{1-k^2}\,L.$$

The relationship between k and the image rejection ratio is given by,

Image rejection ratio [dB] = $-10\log(1-k^2)$.

Next, consider the correlation processing between two stations. The suffixes show each station:

$$U_1' = k_1 U_1 + \sqrt{1-k_1^2}\, L_1$$

$$U_2' = k_2 U_2 + \sqrt{1-k_2^2}\, L_2 .$$

The correlated amplitude ρ is shown as follows:

$$\begin{aligned}\rho &= \langle U_1' U_2' \rangle \\ &= k_1 k_2 \langle U_1 U_2 \rangle + \sqrt{\left(1-k_1^2\right)\left(1-k_2^2\right)}\langle L_1 L_2 \rangle . \end{aligned} \qquad \cdots\cdots\cdots\cdots\cdots\cdots (1)$$

In conventional VLBI, the observed data are affected by Doppler shift caused by the earth's rotation. This is called "fringe rotation". In this case, the second term $<L_1L_2>$ on the right side of Eq. (1) becomes zero because fringe rotation is different between the upper side band and the lower side band. But $<L_1L_2>$ has some correlation in the case of no fringe rotation. The measured image rejection ratio is shown in Fig. 7.

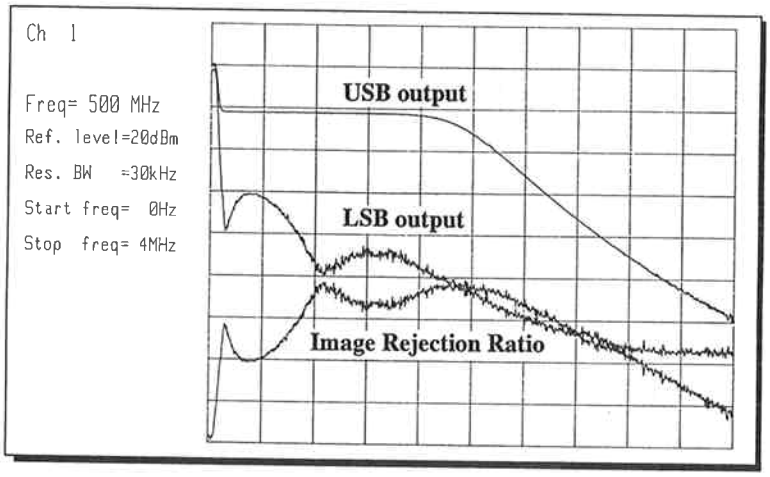

Fig. 7 Image rejection ratio.

If the image rejection ratios for two stations are 19.5 dB and 25 dB, k_1 is 0.9944 (image rejection ratio 19.5 dB) and k_2 is 0.9984 (25 dB). These values are substituted to Eq. (1), then the coherence loss is calculated as follows[9]-[11]:

ρ = 0.72% with fringe rotation,
= 0.12% without fringe rotation.

ii) Phase noise of local signal

Phase noise of the 10 kHz step synthesizer decreases signal coherence. Phase noise is measured by Allan variance. The results are shown in Table 5. This measured phase noise is found to be white noise. Coherence loss (L_c) caused by the instability of the frequency standard is as follows(9)-(11):

$$L_c = \omega_o^2 \left[\frac{\alpha_p}{6} + \frac{\alpha_f T}{12} + \frac{\alpha_y^2 T^2}{57} \right] \qquad \text{(2)}$$

where ω_o = angular frequency of a local oscillator (rad/sec)

α_p = Allan variance of white phase noise at 1 sec

α_f= Allan variance of white frequency noise at 1 sec

σ_y^2 = Allan variance of flicker phase noise

T = integration time in seconds.

Estimated coherence loss caused by phase noise is less than 0.58%.

Table 5 Phase noise of the local oscillator

Phase stability in Allan variance			
	Integration time		
Frequency	1 sec	10 sec	100 sec
100 MHz	$1.4\text{x}10^{-11}$	$1.4\text{x}10^{-12}$	$1.7\text{x}10^{-13}$
200 MHz	$1.4\text{x}10^{-11}$	$1.5\text{x}10^{-12}$	$1.7\text{x}10^{-13}$
300 MHz	$1.2\text{x}10^{-11}$	$1.5\text{x}10^{-12}$	$2.2\text{x}10^{-13}$
400 MHz	$1.4\text{x}10^{-11}$	$1.6\text{x}10^{-12}$	$1.9\text{x}10^{-13}$
500 MHz	$1.5\text{x}10^{-11}$	$1.6\text{x}10^{-12}$	$2.1\text{x}10^{-13}$

iii) Imperfect band pass

There is filter bank in the video converter unit. These filters are 7th order butterworth low pass filters. The loss, β, caused by imperfect band pass can be estimated by the following equation:

$$\beta = \frac{1}{\sqrt{1 + 2\sum_{\tau=1}^{N} R_{11}(\tau) R_{22}(\tau)}}. \qquad \text{(3)}$$

Where $R_{11}(\tau)$ and $R_{22}(\tau)$ are auto-correlation functions of correlated functions after the low pass filter.

iv) Aliasing noise

If under sampling occurs, there is a component whose frequency is more than half of the sampling frequency. The digitized data has some deformation caused by aliasing noise. The coherence loss is defined by β, and it is calculated as follows:

$$\beta = 1 - \frac{\int_0^{\omega_b} P(\omega)d\omega}{\int_0^{2\omega_b} P(\omega)d\omega}. \quad \ldots\ldots\ldots\ldots\ldots\ldots\ldots\ldots\ldots\ldots (4)$$

$P(\omega)$: transfer function
$\omega_b = 2\pi f_c$
f_c = nominal cutoff frequency of low pass filter.

The transfer function of the butterworth filter is described in the next equation:

$$P(f) = \frac{1}{1+(f/f_d)^{2n}}. \quad \ldots\ldots\ldots\ldots\ldots\ldots\ldots\ldots\ldots\ldots (5)$$

n = order of filter
f_d = 3 dB cutoff frequency.

Cutoff frequency fd is selected in order to minimize coherence loss. The selected value is $f_d = 0.91 * f_c$ for $n = 7$.

coherence loss of imperfect band pass = 1.28%
aliasing noise = 1.99%.

4) Sampling

i) Hysteresis

Analog input video signals are digitized (1 bit sampling) by comparators. There is a region of fuzzy digitizing because of offset and hysteresis of the comparator. Assuming that an input signal has a Gausian distribution, and its mean is zero, then the probability of a region of undetermined digitizing is calculated by

$$R(V_o) = 2\int_0^{V_o} \frac{1}{\sqrt{2\pi V_e}} \exp\left[\frac{-V^2}{2V_e^2}\right] dV \quad \ldots\ldots\ldots\ldots\ldots\ldots (6)$$

where V_o = a region of undetermined digitizing
V_e = effective voltage of a signal.

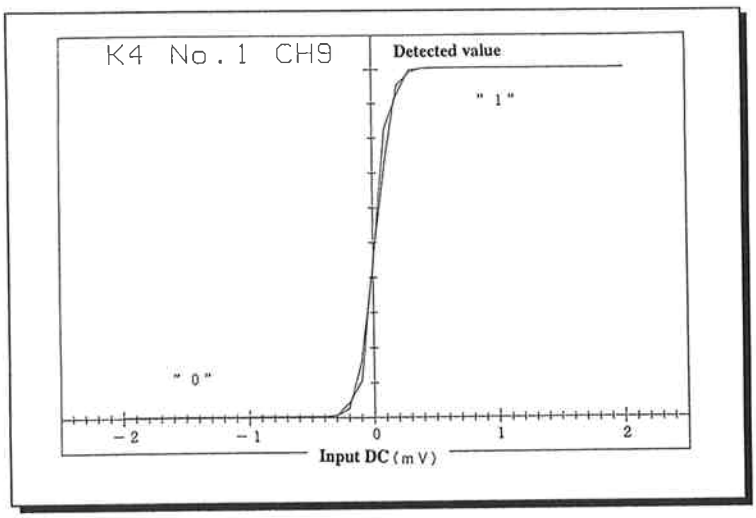

Fig. 8 Characteristic of sampler.

The results for measurement of sampling characteristics are shown in Fig. 8. If input signal power is 0 dBm then $V_e = 0.224\ V$ and V_o is smaller than 2 mV. Coherence loss calculated with Eq. (6) is less than 0.36%.

Next, we discuss the comparator offset. If the probability of a comparated value of "1" from station 1 is $p_1(1)$, then

the probability of "1" and "1"	$P_1 = p_1(1)p_2(1)$
the probability of "1" and "0"	$P_2 = p_1(1)\{1 - p_2(1)\}$
the probability of "0" and "1"	$P_3 = \{1 - p_1(1)\}p_2(1)$
the probability of "0" and "0"	$P_4 = \{1 - p_1(1)\}\{1 - p_2(1)\}$

where $p_1(1)$ = the probability of "1" in data #1 of station 1
$p_2(1)$ = the probability of "1" in data #2 of station 2

For P_1, P_4, the correlation is positive. For P_2, P_3, the correlation is negative. So the output of the count bit M is

$$M = N(P_1 - P_2 + P_3 + P_4)$$
$$= N(2(P_1 + P_4) - 1)$$

where N is total bit.

The correlated value is

$$\frac{M}{N} = 2(P_1 + P_4) - 1. \qquad \ldots\ldots\ldots\ldots\ldots\ldots\ldots\ldots\ldots\ldots\ldots\ldots\ldots\ldots (7)$$

The calculated coherence loss from Eq. (7), in the case of 2 mV DC comparator offset is less than 0.052%. This effect, however, does not affect baseline measurement.

5. Overall Coherence Check of the K-3 and K-4 VLBI Systems

We made an overall coherence check using K-3 and K-4 systems and antenna systems.

5.1 Measurement Method

The block diagram of the measurement system is shown in Fig. 9. Two independent interrelated systems were used: system A and system B. It is possible to change S/N, ratio in order to obtain the relationship between the correlated amplitude and the S/N ratio. The signal source is a noise generator. This signal is divided and injected into system A and system B through a 40 dB directional coupler at the low noise amplifier (LNA) input port. X-band sky noise is used as a noise source for system A and S-band sky noise is used for system B. The coefficient of cross correlation function ρ_o is estimated from the system temperature is as follows:

$$\rho_o = \sqrt{\frac{\{S_1 \cdot S_2\}}{\{(N_1 + S_1)\cdot(N_2 + S_2)\}}} \qquad \ldots\ldots\ldots\ldots\ldots\ldots\ldots\ldots\ldots\ldots\ldots\ldots\ldots\ldots (8)$$

where S_1 = signal temperature in system A
S_2 = signal temperature in system B
N_1 = system noise temperature in system A
N_2 = system noise temperature in system B

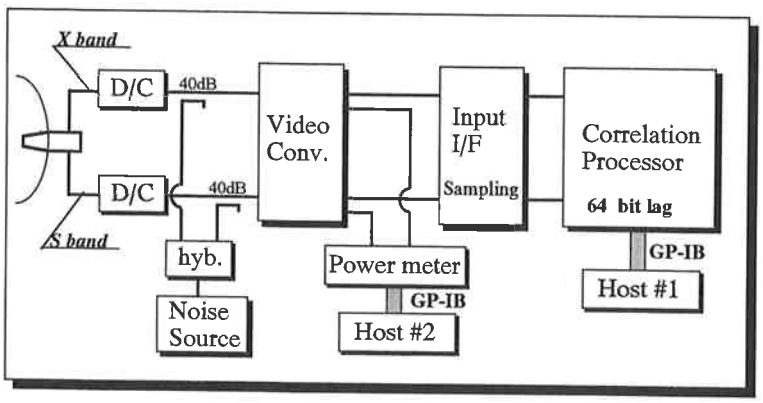

Fig. 9 Overall coherence check block diagram.

The coherence can be estimated by the next equation. ρ_1 is the coefficient of cross correlation function from the correlation processor.

$$\text{coherence loss} = 1 - \frac{\rho_1}{\rho_o}. \qquad \ldots\ldots\ldots\ldots\ldots\ldots\ldots\ldots (9)$$

5.2 Measurement of ρ_1 and ρ_o

ρ_o is calculated from the ratio of detected system noise when the noise source is on to that when it is off. The detected system noise levels, when the noise source is off, are P_1 in system A and P_2 in system B. The detected system noise levels when the noise source is on, are P_3 in system A and P_4 in system B and k is the conversion coefficient from power to noise temperature.

$$N_1 = kP_1$$
$$N_2 = kP_2$$
$$N_1 + S_1 = kP_3$$
$$N_2 + S_2 = kP_4$$

Equation (8) is rewritten as follows:

$$\rho_o = \sqrt{\frac{\{(P_3 - P_1)\cdot(P_4 - P_2)\}}{(P_3 \cdot P_4)}}. \qquad \ldots\ldots\ldots\ldots\ldots\ldots\ldots\ldots (10)$$

It is possible to calculate ρ_1 from the auto-correlation value and the cross-correlation value obtained from the correlation processor. The coherence function $C_o(f)$ is given by

$$C_o(f) = \frac{|S_{xy}(f)|}{\sqrt{S_{xx}(f)\cdot S_{yy}(f)}} \qquad \ldots\ldots\ldots\ldots\ldots\ldots\ldots\ldots (11)$$

where $S_{xx}(f)$ = power spectrum of auto-correlation function of system A
$S_{yy}(f)$ = power spectrum of auto-correlation function of system B
$S_{xy}(f)$ = power spectrum of cross-correlation function between system A and system B.
Total coherence C over the bandwidth B is calculated by

$$C = \frac{1}{B}\int_0^B C_o(f)df. \qquad \ldots\ldots\ldots\ldots\ldots\ldots\ldots\ldots (12)$$

There is difference between correlated amplitude for analog data and for digitized data. Therefore, it is necessary to convert from the obtained correlated value to the real correlated value using the Van Vleck and Middleton's equation. 1 bit sampling correction is made as follows:

$$R(\tau) = \sin\left\{\frac{\pi}{2} r(\tau)\right\} \qquad \ldots\ldots\ldots\ldots\ldots\ldots\ldots\ldots\ldots\ldots\ldots\ldots\ldots\ldots (13)$$

where $R(\tau)$ = real correlated value
$r(\tau)$ = correlated value with 1 bit sampling.

ρ_1 is calculated by as follows:

i) calculate auto-correlation function $r_{xx}(\tau)$ (using 64 bit lag data)
ii) calculate auto-correlation function $r_{yy}(\tau)$ (using 64 bit lag data)
iii) calculate cross-correlation function $r_{xy}(\tau)$ (using 64 bit lag data)
iv) make 1 bit sampling correction
v) find the power spectrum function using Fourier transform (1024 bit)
vi) find the coherence using the coherence function.

ρ_1 is larger than ρ_o because the K-3 correlation processor does not suppress correlation during header data. The relationship between ρ_1 and ρ_o is shown in Fig. 10. ρ_1/ρ_o shows coherence. If ρ_1/ρ_o is 1, then coherence is 1. Here, a value of 0.975 was obtained for ρ_1/ρ_o. The overall coherence loss was 2.5% at 250 MHz, but that does not include the loss due to aliasing noise in the case where there was no fringe rotation. Table 6 shows a summary of coherence loss as discussed above.

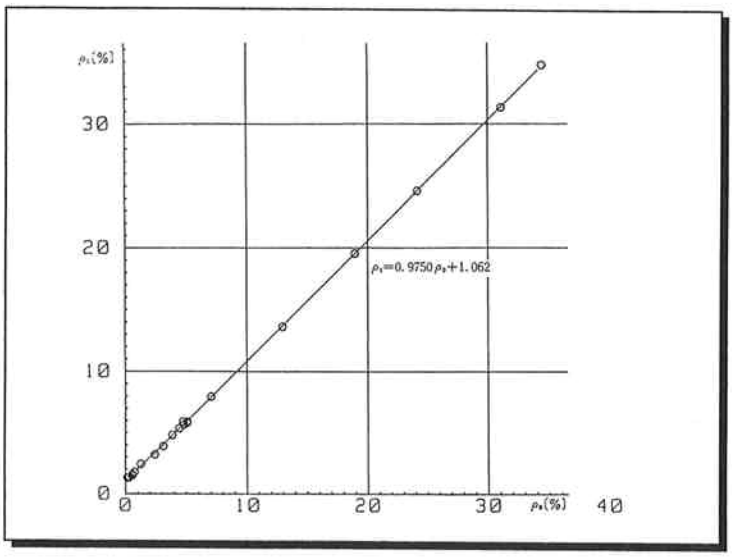

Fig. 10 Overall coherence loss.

The estimated total coherence loss is less than 5% in K-3 and K-4 VLBI data acquisition systems, but this value does not include the correlation processing loss or the atmosphere loss, fringe stopping, phase scintillation etc.

Table 6 The summary of coherence loss

Estimated Loss in worst case		
Coherence Loss Factors	**Fringe Rotation**	**Without Fringe Rotation**
Local Phase Noise (3.1 deg.)	**0.23 %**	**0.23 %**
Imperfect Image rejection (23dB)	**0.72 %**	**0.12 %**
Imperfect Filtering	**1.28 %**	**1.28 %**
Aliasing Loss	**1.99 %**	———
Clipping Loss	**0.36 %**	**0.36 %**
Total	**4.58 %**	**1.99 %**

We estimated the coherence of the K-3 and K-4 system. The measured coherence loss of the K-3 and K-4 systems was less than 5%. This shows that the K-3 and K-4 systems perform well enough for the VLBI experiments.

6. Performance Check for K-4 System

A domestic VLBI experiment between Kashima and Tsukuba was carried out on June 15, 1989. In this experiment, the K-3 and K-4 acquisition systems were used to compare the results and the

Table 7 The results of baseline analysis for the Kashima-Tsukuba VLBI experiment

	K-3 system		*K-4 system*		
	Length in [m]	σ in [m]	Length in [m]	σ in [m]	Difference in [m]
X element	40719.331	0.020	40719.327	0.019	-0.004
Y element	33656.704	0.017	33656.713	0.016	0.009
Z element	13590.709	0.022	13590.716	0.018	0.007
Baseline Length	54548.556	0.007	54548.561	0.005	0.005

performances at both stations. It was found that the geodetic results from the K-4 system agreed with those from the K-3 system, within only a few millimeters in vector. The results are tabulated in Table 7. The residual delay is 0.091 nsec and the residual rate is 0.151 ps/s. These results show that the K-4 system gives better performance than the K-3 system. Moreover, only 8 medium size cassette tapes were used for a 24 hours experiment with the K-4 system whereas 30 tapes were needed for the same experiment with the K-3 system. It is possible to perform this experiment with only 3 or 4 of large size tapes.

7. Conclusion

The measured coherence loss for both K-4 and K-3 systems is less than 5%. This shows that the K-4 and K-3 systems perform well enough for the VLBI experiments. Geodetic results on the 55 km baseline (Kashima-Tsukuba) using the K-4 system agreed with those of the K-3 system with only a few millimeters of difference in vector. The K-4 system has already been used for domestic VLBI experiments on remote islands and for Antarctic VLBI experiment.

Acknowledgement

We would like to express our thanks to staff of SONY and Nihon Tsushinki Co. and staff of Kashima Space Research Center.

We are indebted to the staff members of the Geographical Survey Institute for assistance with the domestic experiments.

References

(1) Kraus, J. D., Radio Astronomy, McGraw-Hill, 1966.

(2) Whitney, A. R., "Precision geodesy and astrometry via Very-Long Baseline Interferometry", Doctor Thesis at the Massachusetts Institute of Technology, Jan. 1974.

(3) Hinteregger, H. F., I. I. Shapiro, D. S. Robertson, C. A. Knight, R. A. Ergas, A. R. Whitney, A. E. E. Rogers, J. M. Moran, T. A. Clark, and B. F. Burke, "Precision Geodesy via Radio Interferometry," SCIENCE, **178**, 396–398, Oct. 1972.

(4) Whitney, A. R., H. F. Hinteregger, C. A. Knight, J. I. Levine, S. Lippinct, T. A. Clark, I. I. Shapiro, and D. S. Robertson, "A very-long-baseline interferometer system for geodetic applications," Radio Science, **11**, 5, 421–432, May 1976.

(5) Hama, S., T. Yoshino, H. Kiuchi, T. Morikawa, T. Sato, T. Shiomi, F. Takahashi, and W. J. Klepczynski, "First International Time and Frequency Comparison Experiment by using Very Long baseline Interferometry", J. Radio Res. Lab., **34**, 142, Jul. 1987.

(6) Kiuchi, H., J. Amagai, S. Hama, T. Yoshino, N. Kawaguchi, and N. Kurihara, "Instrumental Delay Calibration by Zero Baseline Interferometry for International VLBI Time Comparison," J. Radio Res. Lab., **34**, 143, Nov. 1987.

(7) Mark-III Documentation

(8) Rogers, A. E. E., "Very Long Baseline Interferometry with effective band width for phase-delay measurements," Radio Science, **5**, 10, 1239–1247, Oct. 1970.

(9) Rogers, A. E. E., "The sensitivity of a very long baseline interferometer," Radio Interferometry Techniques for Geodesy, NASA Conference Publication 2115, 1980.

(10) Rogers, A. E. E., "Coherence Limits for Very-Long-Baseline Interferometry," IEEE trans., IM-

30, **4**, 283–286, Dec. 1981.

(11) Kawaguchi, N., "Coherence loss and Delay Observation Error in Very-Long-Baseline Interferometry," J. Radio Res. Lab., **30**, 129, Mar. 1983.